FUNCTION™ american physiological society

FUNCTION, 2022, 3(4): zqac022

https://doi.org/10.1093/function/zqac022
Advance Access Publication Date: 30 April 2022
Original Research

RESEARCH ARTICLE

Multimodality Deep Phenotyping Methods to Assess Mechanisms of Poor Right Ventricular–Pulmonary Artery Coupling

Farhan Raza [1,*], Callyn Kozitza [2], Chris Lechuga [3], Daniel Seiter [4], Philip Corrado [4], Mohammed Merchant [1], Naga Dharmavaram [1], Claudia Korcarz [1], Marlowe Eldridge [5], Christopher Francois [6], Oliver Wieben [3], Naomi Chesler [4]

[1]Department of Medicine, Cardiovascular Division, University of Wisconsin-Madison, Wisconsin, USA, [2]Biomedical Engineering, University of Wisconsin-Madison, Wisconsin, USA, [3]Edwards Lifesciences Foundation Cardiovascular Innovation and Research Center and Department of Biomedical Engineering, University of California, Irvine, USA, [4]Medical Physics, University of Wisconsin-Madison, Wisconsin, USA, [5]Department of Pediatrics, University of Wisconsin-Madison, Wisconsin, USA and [6]Department of Radiology, Mayo Clinic, Rochester MN, USA

*Address correspondence to F.R. (e-mail: fraza@medicine.wisc.edu)

Abstract

Deep phenotyping of pulmonary hypertension (PH) with multimodal diagnostic exercise interventions can lead to early focused therapeutic interventions. Herein, we report methods to simultaneously assess pulmonary impedance, differential biventricular myocardial strain, and right ventricular:pulmonary arterial (RV:PA) uncoupling during exercise, which we pilot in subjects with suspected PH. As proof-of-concept, we show that four subjects with different diagnoses [pulmonary arterial hypertension (PAH); chronic thromboembolic disease (CTEPH); PH due to heart failure with preserved ejection fraction (PH-HFpEF); and noncardiac dyspnea (NCD)] have distinct patterns of response to exercise. RV:PA coupling assessment with exercise was highest-to-lowest in this order: PAH > CTEPH > PH-HFpEF > NCD. Input impedance (Z_0) with exercise was highest in precapillary PH (PAH, CTEPH), followed by PH-HFpEF and NCD. Characteristic impedance (Z_C) tended to decline with exercise, except for the PH-HFpEF subject (initial Zc increase at moderate workload with subsequent decrease at higher workload with augmentation in cardiac output). Differential myocardial strain was normal in PAH, CTEPH, and NCD subjects and lower in the PH-HFpEF subject in the interventricular septum. The combination of these metrics allowed novel insights into mechanisms of RV:PA uncoupling. For example, while the PH-HFpEF subject had hemodynamics comparable to the NCD subject at rest, with exercise coupling dropped precipitously, which can be attributed (by decreased myocardial strain of interventricular septum) to poor support from the left ventricle (LV). We

Submitted: 18 January 2022; **Revised:** 1 April 2022; **Accepted:** 20 April 2022

conclude that this deep phenotyping approach may distinguish afterload sensitive vs. LV-dependent mechanisms of RV:PA uncoupling in PH, which may lead to novel therapeutically relevant insights.

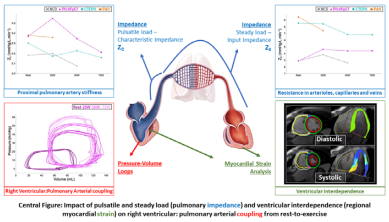

Central Figure: Impact of pulsatile and steady load (pulmonary impedance) and ventricular interdependence (regional myocardial strain) on right ventricular: pulmonary arterial coupling from rest-to-exercise

Key words: pulmonary impedance; right ventricular pressure volume loops; RV:PA uncoupling; exercise hemodynamics; myocardial strain

Introduction

Right ventricular (RV) failure is a predictor of adverse outcomes in left heart failure and pulmonary hypertension (PH).[1]The precursor of RV failure is uncoupling of the right heart:pulmonary arterial (PA) hemodynamic unit.[2] However, RV:PA uncoupling can occur due to distinct mechanisms, including increased RV afterload and left heart failure, which can impair RV function through ventricular interdependency.[3,4] In highly heterogeneous populations such as those with heart failure with preserved ejection fraction (HFpEF), clinically complex methods that use multiple modalities to collect robust ventricular and pulmonary vascular function data, ie, deep phenotyping, may help identify limitations and mechanisms of RV:PA uncoupling, leading to early diagnosis and focused interventions.

Robust measurement of RV:PA coupling requires collection of simultaneous pressure–volume data.[5,6] Pulmonary vascular function is best assessed with pulmonary vascular impedance, which accounts for the opposition of the pulmonary circulation to pulsatile flow.[6] Ventricular function and especially ventricular interdependency can be measured via myocardial strain analysis.[7] The use of these three methods during exercise in subjects with different PH phenotypes (pre or postcapillary) has not been reported.

Methods

We recruited adult subjects with NYHA class II dyspnea. Participants were excluded for: left ventricular ejection fraction < 50%, cardiac amyloidosis, lung parenchymal disease requiring supplemental oxygen, contraindications to MRI, an implanted pacemaker or defibrillator, unstable cardiac problems (angina or arrhythmias), acute infectious illness, or hospitalization within the prior 3 mo. The study was approved by the University of Wisconsin-Madison institutional review board (ID: 2019–1184) and complied with the guidelines of Declaration of Helsinki.

A total of four subjects were enrolled; they had post-testing diagnoses of pulmonary arterial hypertension (PAH), chronic thromboembolic disease (CTEPH), PH due to HFpEF (PH-HFpEF), and noncardiac dyspnea (NCD). Subjects underwent invasive cardiopulmonary exercise testing (iCPET) in a semirecumbent position, as previously described.[8] A 3Fr right radial arterial line was placed, and two venous sheaths were placed in the right internal jugular vein with a 7Fr fluid-filled pressure catheter and a 4Fr high fidelity (Millar) PA pressure catheter (Figure 1A). Full echocardiogram with measurement of RV outflow tract (RVOT) diameter was performed at rest, and pulse wave Doppler images of the RVOT were obtained during iCPET. At different stages (rest followed by exercise stages held at every 25 watts until peak exercise, and 5-min into recovery), simultaneous RVOT images (for velocity and derived flow) and PA pressure measurements were obtained for spectral analysis. Pressure–volume loops were collected with a 7F conductance catheter (CD Leycom, Zoetermeer, the Netherlands) inserted near the RV apex and adjusted until counterclockwise loops were noted in the majority of the 7 individual electrode pairs (electrodes with clockwise loops were excluded; Figure 1B). The loop-width was matched to direct Fick cardiac output and stroke volume. RV volumes derived from cardiac MRI were used for volume calibration. Real-time pressure–volume loops were obtained at rest, similar exercise stages and recovery (Figure 1C).

Cardiac magnetic resonance imaging (cMRI; Discovery MR750, GE Healthcare, Waukesha, WI) was performed within 24-h of catheterization to assess myocardial function, strain, and 4D flow at rest and during exercise. Exercise was performed in the magnet bore with a pneumatic MRI-compatible exercise stepper (Cardio Step Module; Ergospect, Innsbruck, Austria). Target exercise power for each participant was based on 70% of maximal heart rate achieved during the iCPET.

Synchronized PA pressure and flow were used to determine pulmonary vascular impedance as the ratio of pressure to flow moduli.[6] After RVOT area was estimated for each subject at each level of exercise (dividing Fick-derived stroke volume by echocardiogram-derived velocity time integral), input impedance (Z_0), characteristic impedance (Z_C), and pulse wave reflection were calculated as described previously.[9] A second derivative single-beat pressure method was used to calculate RV:PA coupling.[10] In addition, coupling was estimated using the pressure-only method.[10] Tau was calculated as the time from dP/dt min until pressure reaches half the value at dP/dt min. EDPVR was determined with the single beat method described by Klotz et al.[5] in which data are fit to $EDP = \alpha \cdot EDV^{\beta}$, where α is a curve fitting parameter and β is the diastolic stiffness.

Using 2D gray scale images, speckle tracking angle-independent Velocity Vector Imaging (VVI; Siemens, Erlangen, Germany) analysis was carried out to measure 2D strain from echocardiogram. Left ventricle (LV) peak global longitudinal strain was computed by averaging 4- and 2-chamber views. RV free wall peak longitudinal strain was evaluated. The average frame rate of the clips for RV and LV strain analysis was 30–50 Hz. Analysis of cMRI images was performed using a commercially available software (cvi42, version 5.6.6; Circle Cardiovascular Imaging Inc). Ventricular volumes were calculated from short-axis, cine-balanced, SSFP series. Three slices from the LV and the RV (base, mid, and apex) short-axis and long-axis cine MRI scans were used to analyze longitudinal, circumferential, and radial dimensions and strain as a function of time, including average peak strain and systolic and diastolic strain rate, as previously described.[7]

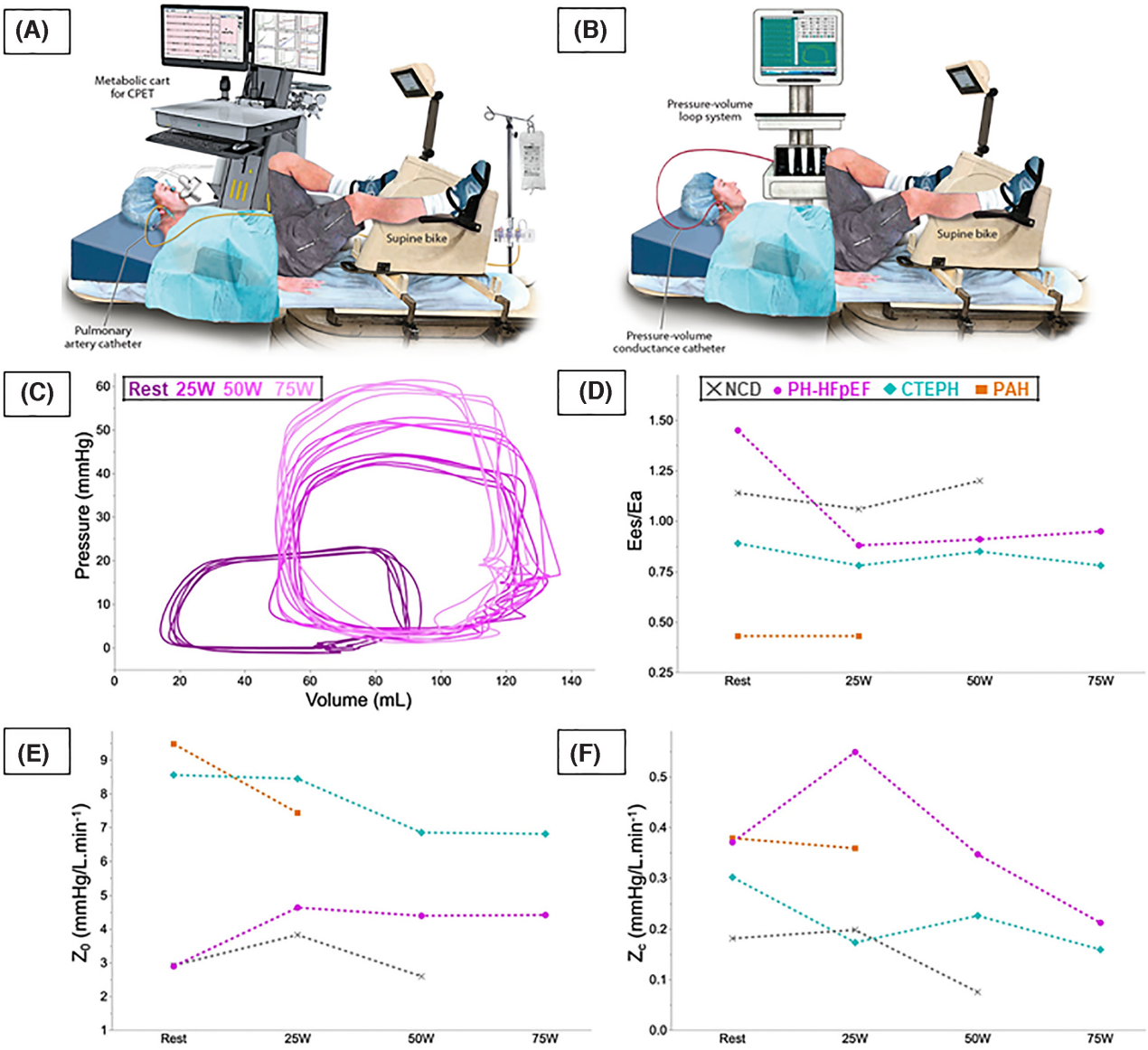

Figure 1. Representative figure of methodology and subject phenotypes. (A) and (B). Invasive cardiopulmonary exercise test and right ventricular pressure–volume loops, at rest and with exercise. (C) Representative pressure volume loops for PH-HFpEF subject. (D) RV:PA coupling at rest and different levels of exercise (end systolic elastance: Ees to effective arterial elastance: Ea ratio). (E) Input impedance (Z_0) at rest and with exercise. (F) Characteristic impedance (Z_C) at rest and with exercise.

Results

The table 1 summarizes the baseline characteristics, hemodynamic data, and myocardial strain data. Subjects were between the age of 63 and 70-years-old, and BMI range of 23–34. Echocardiographic features included: RV:LV ratio 0.9–1.0, eccentricity index < 1.1, peak tricuspid regurgitant velocity 2.0–2.8 m/s, and systolic RV base/apex ratio > 1.5.[11]

While the PH-HFpEF subject had the highest RV:PA coupling (Ees: Ea) at rest, with exercise Ees: Ea was highest-to-lowest in this order: PAH > CTEPH > PH-HFpEF > NCD (Figure 1D). At rest, the input impedance (Z_0) was higher in the precapillary phenotypes (CTEPH and PAH), and lower in PH-HFpEF and NCD subjects, as expected. With exercise, Z_0 was highest-to-lowest in this order: CTEPH > PAH > PH-HFpEF > NCD (Figure 1E). At rest, the characteristic impedance (Z_C) was similar among all subjects and tended to decline with exercise except for the PH-HFpEF subject, for whom, Z_C increased at a moderate workload and then decreased (Figure 1F). The differential myocardial strain analysis of global LV, interventricular septum and the RV free wall provided insights in LV–RV interactions (Table 1). In particular, the interventricular septal strain was lowest in the PH-HFpEF subject, which may indicate poor contribution of LV to RV contractility via moderator band.

The degree of exercise limitation, as defined by peak VO_2 achieved, was severe for the PAH subject (45%), while mild-moderate for the CTEPH (74%) and PH-HFpEF (65%) subject. The NCD subjects had a mild limitation (78%) per actual body weight (79 kg, BMI 34). However, if indexed to ideal body weight, her peak VO_2 was 96% (24.3 mL/kg/min). This indicated that a predominant cause of exercise limitation was related to obesity.

Table. 1. Baseline characteristics, hemodynamics, and myocardial strain

Subject	1		2		3		4	
Diagnosis	**PAH**		**CTEPH**		**PH-HFpEF**		**NCD**	
Age	70		66		66		63	
Sex	F		F		M		F	
BMI (kg/m^2)	23.6		25.7		25.1		34.0	
KCCQ-23 score	52		80		62		96	
BNP (pg/mL)	134		91		112		40	
Hemodynamics (rest, exercise)								
	Rest	Ex	Rest	Ex	Rest	Ex	Rest	Ex
A. Pressure–volume loop data								
Ees (mmHg/mL)	0.32	0.51	0.86	0.91	0.39	0.60	0.47	0.69
Ea (mmHg/mL)	0.76	1.20	0.97	1.17	0.27	0.63	0.41	0.57
Ees:Ea	0.43	0.43	0.89	0.78	1.45	0.95	1.14	1.20
EDPVR (mmHg/mL)	0.04	0.09	0.11	0.13	0.02	0.14	0.04	0.06
EDPVR single beat method, β (·)	5.6	5.8	5.8	5.9	5.5	6.3	5.7	5.8
Tau (m/s)	37	37	40	27	26	30	36	38
RVEF (%) ‡	58.1	48.6	47.5	50.8	66.7	55.7	61.5	69.2
B. Impedance data								
Z_c (mmHg/L/min)	0.38	0.36	0.30	0.16	0.37	0.21	0.18	0.07
Z_0 (mmHg/L/min)	9.5	7.4	8.6	6.8	2.9	4.4	2.9	2.6
C. Invasive CPET test data								
CPET								
Peak VO_2 [mL/kg/min], (%)	8.9 (45%)		16.2 (74%)		16.0 (65%)		16.9 (78%)	
Peak O_2 pulse (mL/beat)	6.7		16.2		12.7		14.4	
Peak watts (W)	30		100		110		75	
RER	1.05		1.02		1.07		1.20	
Peak V_E/VCO_2	43		36		34		25	
Peak $ETCO_2$ (mmHg)	29		34		31		41	
Breathing reserve (%)	74		65		54		55	
Rest hemodynamics								
Rest heart rate	68		71		56		88	
Rest RAP (mmHg)	12		11		6		6	
Rest PAP (mmHg)	70/27 (38)		34/19 (26)		23/12 (15)†		26/12 (18)	
Rest PAWP (mmHg)	12		12		10		10	
Rest cardiac output (L/min)	3.95		3.38		4.69		6.03	
Rest stroke volume Index (mL/m^2)	37.5		26.8		42.5		39.0	
Rest PVR (WU)	6.6		4.1		1.1		1.3	
Exercise hemodynamics								
Peak heart rate	85		129		84		121	
Peak RAP (mmHg)	12		17		14		16	
Peak PAP (mmHg)	78/28 (48)		76/40 (54)		56/26 (34)		36/23 (29)	
Peak PAWP (mmHg)	15		20		26		18	
Peak cardiac output (L/min)	7.15		9.25		9.40		12.60	
Peak stroke volume index (mL/m^2)	54.3		40.3		56.8		59.2	
mPAP/CO slope (mmHg/L/min)	3.4		5.3		5.2		2.1	
Exercise TPR (mmHg/L/min)	6.7		5.8		3.6		2.3	
PAWP/CO slope (mmHg/L/min)	0.9		1.7		2.8		1.5	
Distensibility (%/mmHg)	0.71		0.53		0.63		0.84	
Myocardial strain analysis								
A. Cardiac MRI radial strain								
Global LV (%)	38.1		27.8		22.3		30.6	
IVS (%)	24.1		15.6		12.7		30.0	
RV free wall (%)	15.5		17.2		31.2		45.0	
B. Echocardiogram								
Global LV (%)	−19.1		−19.2		−16.0		−16.5*	
IVS (%)	−19.3		−19.6		−14.8		−16.7*	
RV free wall (%)	−28.4		−22.6		−18.8		−22.4*	

Peak exercise stage for subjects: #1 25W, #2 75, #3 75, and #4 50.

*Mild obesity contributing to limitation of image quality.

†Exercise hemodynamics: PAP 61/26 (42) PAWP 26 CO 9.68.

‡ Rest cardiac MRI data used for volume calibration for rest pressure volume-loop data.

Abbreviations: PAH: pulmonary arterial hypertension, CTEPH: chronic thromboembolic pulmonary hypertension, PH-HFpEF: pulmonary hypertension due to heart failure with preserved ejection fraction, NCD: noncardiac dyspnea, BMI: body mass index, KCCQ: Kansas City Cardiomyopathy Questionnaire, BNP: Brain natriuretic peptide, Ex: exercise, Ees: end-systolic elastance, Ea: effective arterial elastance, EDPVR: end-diastolic pressure volume relationship, Tau: time constant of RV relaxation, RVEF: right ventricular ejection fraction, Z_c: characteristic impedance, Z_0: input impedance, CPET: cardiopulmonary exercise test, VO_2: oxygen consumption, RER: respiratory exchange ratio, V_E/VCO_2: minute ventilation-carbon dioxide slope, $ETCO_2$: end-tidal pressure of carbon dioxide, RAP: right atrial pressure, PAP: pulmonary artery pressure, PAWP: pulmonary artery wedge pressure, PVR: pulmonary vascular resistance, CO: cardiac output, TPR: transpulmonary resistance, LV: left ventricle, IVS: interventricular septum, and RV: right ventricle.

Discussion

With the significant caveat that only four subjects were included, the combination of iCPET, pulmonary vascular impedance, and pressure–volume loops analysis at rest and with exercise suggests deep phenotyping may identify differences in limitations and mechanisms of RV:PA uncoupling. The PH-HFpEF subject, eg, had hemodynamics comparable to the NCD subject at rest but, with exercise, coupling dropped precipitously as Z_0 and Zc increased sharply (at 25 W) and thereafter, while coupling and Z_0 held steady, Zc decreased to rest values. Contributing to decreased coupling, left ventricular support of RV function likely diminished with exercise as evidenced by decreased myocardial strain of the interventricular septum (Table 1). We interpret the initial increase and then decrease in Zc as pressure-induced proximal PA stiffening followed by dilation to accommodate increased cardiac output. In comparison to this PH-HFpEF subject, in both precapillary PH subjects, the RV is poorly coupled at rest and exercise in response to sustained increases in Z_0 since left ventricular support is intact. In NCD, RV:PA coupling is preserved at rest and with exercise due to a low afterload (Ea and Z_0 low at rest) and decreasing Z_C (with exercise) and preserved myocardial strain.

Conclusion

Thus, deep phenotyping methods, or the combination of multimodal approaches such as presented here, may subphenotype current clinical PH classifications (based on rest imaging and hemodynamics). In doing so, these methods with exercise testing may yield novel therapeutically relevant insights that justify the clinical complexity of data collection.

Funding

This study was supported from the UW-Madison Department of Medicine (DOM) pilot fund (233-AAH9756), and the National Heart, Lung, and Blood Institute of the National Institutes of Health (Award Number T32HL116270). The content is solely the responsibility of the authors and does not necessarily represent the official views of the National Institutes of Health.

Acknowledgments

We would like to acknowledge our staff at the UW-Madison cardiac catheterization laboratory for maintaining the invasive cardiopulmonary exercise test laboratory: Mary Sue Ireland, Scott Wessels, Chantel Nelson, and Holly Studier. We would also like to acknowledge Joe Chovan (medical illustrator).

Authors' Contributions

The study was conceived and designed by N.C., F.R., C.F., O.W., and M.E. F.R., D.S., and Cl.K. collected the data. Ca.K., C.L., and N.C. analyzed the pulmonary impedance and right ventricular pressure–volume loop data. D.S., P.C., M.M., N.D., and O.W. processed the MRI images and performed myocardial strain analysis on MRI. F.R. performed the myocardial strain analysis on echocardiographic images. F.R., C.K., C.L., and N.C. reviewed the data and performed analysis. F.R., C.K., and N.C. formulated and wrote the manuscript. All co-authors reviewed, edited, and approved the manuscript before submission.

Conflict of Interest

The authors declare that there are no conflict of interests.

Data Availability

The data underlying this article will be shared on reasonable request to the corresponding author.

References

1. Haddad F, Doyle R, Murphy DJ, Hunt SA. Right ventricular function in cardiovascular disease, part II: pathophysiology, clinical importance, and management of right ventricular failure. *Circulation*. 2008; **117**(13):1717–1731. DOI: 10.1161/CIRCULATIONAHA.107.653584.
2. Vanderpool RR, Pinsky MR, Naeije R, et al. RV-pulmonary arterial coupling predicts outcome in patients referred for pulmonary hypertension. *Heart*. 2015;**101**(1): 37–43.
3. Saouti N, Westerhof N, Postmus PE, Vonk-Noordegraaf A. The arterial load in pulmonary hypertension. *Eur Respir Rev*. 2010;**19**(117):197–203.
4. Marcus JT, Gan CTJ, Zwanenburg JJM, et al. Interventricular mechanical asynchrony in pulmonary arterial hypertension. Left-to-right delay in peak shortening is related to right ventricular overload and left ventricular underfilling. *J Am Coll Cardiol*. 2008;**51**(7):750–757.
5. Klotz S, Dickstein ML, Burkhoff D. A computational method of prediction of the end-diastolic pressure-volume relationship by single beat. *Nat Protoc*. 2007;**2**(9):2152–2158.
6. Bellofiore A, Dinges E, Naeije R, et al. Reduced haemodynamic coupling and exercise are associated with vascular stiffening in pulmonary arterial hypertension. *Heart*. 2017;**103**(6):421–427.
7. Sato T, Ambale-Venkatesh B, Zimmerman SL, et al. EXPRESS: right ventricular function as assessed by cardiac magnetic resonance imaging-derived strain parameters compared to high-fidelity micromanometer catheter measurements. *Pulmon Circul*. 2021:**11**(4):1–10. DOI: 10.1177/20458940211032529.
8. Kozitza CJ, Tao R. Pulmonary vascular distensibility with passive leg raise is comparable to exercise and predictive of clinical outcomes in pulmonary hypertension. *Circ Heart Fail*. 2022:**9**(6):1–10. DOI: 10.1002/pul2.12029.
9. Oakland HT, Joseph P, Naeije R, et al. The arterial load and right ventricular-vascular coupling in pulmonary hypertension. *J Appl Physiol*. 2021;**131**(March):424–433.
10. Bellofiore A, Vanderpool R, Brewis MJ, Peacock AJ, Chesler NC. A novel single-beat approach to assess right ventricular systolic function. *J Appl Physiol*. 2018;**124**(2): 283–290.
11. Raza F, Dillane C, Mirza A, et al. Differences in right ventricular morphology, not function, indicate the nature of increased afterload in pulmonary hypertensive subjects with normal left ventricular function. *Echocardiography*. 2017;**34**(11):1584–1592.